Zeitschrift für Kristallographie, Bd. 130, S. 68–87 (1969)

The crystal structure of a disordered epistilbite

By M. SLAUGHTER and W. T. KANE[1]

Department of Geology, University of Missouri, Columbia

(Received 27 May 1968)

Auszug

Die Gitterkonstanten des Epistilbits sind $a = 9{,}04$, $b = 17{,}73$, $c = 9{,}08$ Å, $\beta = 111°50'$; die Raumgruppe ist $C2$. Die Struktur ist aus fünfgliedrigen Ringen von SiO_4-Tetraedern aufgebaut. Durchgehende Kanäle durch achtgliedrige Ringe werden unter rechten Winkeln von versetzten Kanälen durch zehngliedrige Ringe geschnitten. In den Schnittpunkten befinden sich die C-Atome; sie sind umgeben von fünf Wassermolekülen und drei Gerüst-Sauerstoffatomen und verteilen sich regellos auf zwei Lagen der Raumgruppe $C2/m$, wobei die Regellosigkeit anscheinend auf mehr oder weniger zufälliger Verschiebung von Reihen von Ca-Ionen parallel [101] beruht. Der Ersatz von Si durch Al hängt eng mit der Lage der C-Atome zusammen.

Abstract

The zeolite epistilbite is monoclinic, $a = 9.04$, $b = 17.73$, $c = 9.08$ Å, $\beta = 111°50'$, space group $C2$. The structure is built of five-membered rings of Si tetrahedra. Continuous 8-membered-ring channels are intersected at right angles by staggered, narrow 10-membered-ring channels. Ca ions occupy channel intersections and are surrounded by five water molecules and three framework oxygen atoms to form a distorted square antiprism. Calcium ions are disordered on two sites in $C2/m$, the disordering apparently occurring as more or less random shifts of rows of calcium ions parallel to [101]. Aluminum substitution for silicon correlates closely with Ca positions.

Introduction

Epistilbite, a member of the laminar zeolite family, is related to mordenite, dachiardite and the more common zeolites heulandite and stilbite. The importance of epistilbite lies in the relationship of its properties to those of other zeolites. For example, epistilbite is a poor cation exchanger relative to heulandite but compositionally they are similar. Even though the composition of epistilbite is similar to more

[1] Present address: Corning Research Laboratories, Corning, New York.

widely occurring zeolites such as heulandite and stilbite, its presence has been noted at few localities and one would presume that the epistilbite structure is a response to special energy conditions.

We have determined the structure of a disordered epistilbite to relate its structure to the ordered epistilbite and the structures of other common rock-forming zeolites. The crystal structure was also expected to provide information for understanding the mechanics of ion exchange in epistilbite and energy relations among the family of laminar zeolites.

Two structures of epistilbite were presented simultaneously[2], one by PERROTA and one by us. The Perrota structure differed in several respects from ours, their structure being ordered and of higher symmetry. Their structure probably represents a nearly ideal epistilbite.

The crystal-cell data for epistilbite are: $(Ca_{2.59}Na_{1.06}K_{0.10}) \cdot (Al_{8.29}Si_{17.71}O_{48}) \cdot 15.74\,H_2O$; $C2/m$; $a = 9.08$, $b = 17.74$, $c = 10.25$; ± 0.01 Å; $\beta = 124.54° \pm 0.05°$). The structure was determined by three-dimensional least-squares methods by PERROTTA (1967). The alumino-silicate framework was found to be composed of 4-, 5-, and 8-membered rings of tetrahedra. There were two sets of intersecting channels, each defined by 8-membered rings. The (Ca,Na) atoms in the channels were found to be in contact with seven water molecules and two oxygen atoms, giving a coordination of nine at a cut-off distance of 2.77 Å. Partial Al—Si ordering exists with one tetrahedron occupied preferentially by aluminum. This tetrahedron contained the two oxygen atoms that are coordinated with the (Ca,Na) atom. Cations of (Ca,Na) occupy one site only and the water positions are clearly defined about the Ca position. No streaking was observed on Weissenberg photographs (PERROTTA, personal communication).

Experimental

Morphology and optical data

The epistilbite crystals used in the x-ray analysis were supplied by the United States National Museum through Col. CLARENCE M. JENNI. Dr. G. P. L. WALKER collected them near Tiegarhon, Berufjord, Iceland.

The crystals were complexly intergrown and twinned, forming irregular, colorless, translucent to transparent, tabular laths. Translucent crystals with even slight clouding were complexly intergrown

[2] National Meeting of American Crystallographic Assoc., June, 1965.

multiples unsuitable for x-ray analysis. Sparse transparent roof-shaped twins provided the crystals used for analysis. Transparent twinned crystals had no natural faces but a single well developed cleavage plane was regularly present.

The following optical properties were determined:

$n_a = 1.500,\ n_b = 1.511,\ n_c = 1.513,\ 2V = 40°,\ r > v$ strong.

Chemical composition

A chemical analysis by Booth, Garret and Blair, Inc., yielded the following results:

Oxides	Weight %
SiO_2	57.00
Al_2O_3	17.99
CaO	8.31
K_2O	0.20
Na_2O	1.48
MgO	0.01
SrO	0.06
FeO	—
Fe_2O_3	—
TiO_2	—
H_2O^+	14.46
H_2O^-	2.32
Total	101.83

The cell formula for this epistilbite is as follows:

$$Ca_{2.74}Na_{.44}K_{.03}Mg_{.05}Al_{6.52}Si_{17.57}O_{48} \cdot 15H_2O.$$

This aggrees closely with an analysis of epistilbite from the same locality quoted by STRUNZ and TENNYSON (1956).

Observed and calculated density

The density of epistilbite, determined by the Berman density balance, is $2.239 \pm .005$ g/cm³. The calculated density, 2.215 g/cm³, was computed from the experimental value of 1362.7 Å³ for the volume of the unit cell and its chemical formula. Both the observed and calculated values of density are close to the value of $\simeq 2.2$ given by DEER, HOWIE and ZUSSMAN (1963, p. 377).

Differential-thermal analysis

A differential-thermal analysis was performed on epistilbite using a Robert L. Stone instrument. The sample, ground for thirty minutes in a power mortar, was heated at a rate of 12.3 °C per minute to 1000 °C. The thermogram (Fig. 1) exhibits a moderate endothermic peak at about 150 °C, probably due to loss of adsorbed and absorbed

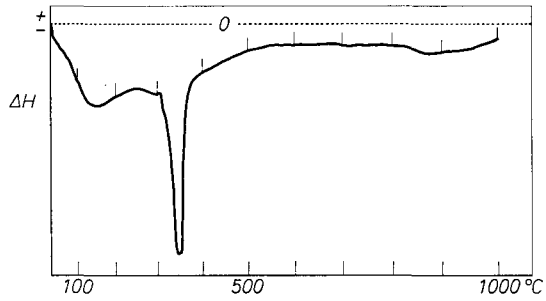

Fig. 1. Differential-thermal analysis pattern of epistilbite. Lowest temperature absorption peak corresponds to loss of water bound to the framework. Sharp absorption peak corresponds to loss of water bound to Ca ions

water. A strong endothermic peak at 350 °C reflects the expulsion of water tightly bound to Ca cations. The thermogram remains slightly endothermic to 1000 °C with no significant peaks.

Powder data and collection of x-ray single-crystal intensities

An x-ray powder diffractogram was made from the material used in this study. Observed and calculated spacings and indices are given in Table 1.

Intensity measurements were made by means of a Buerger-Supper single-crystal diffractometer with Ni-filtered Cu$K\alpha$ radiation. Data were taken from ten levels for crystal rotation around the c axis, with overlapping data collected about the a axis. A total of 1053 independent reflections was measured around the c axis; 32 reflections were rejected as unreliable. The diffractometer data were scaled for counter losses, and corrected for absorption and Lorentz-polarization effects.

The Weissenberg photographs exhibited pronounced disorder streaks associated with the 602, 404 and 206 reflections.

Table 1. *Powder-diffraction data for epistilbite*

d_{obs}	d_{calc}	I_{obs}	hkl
8.84 Å	8.864 Å	57	020
8.453	8.453	2	110
6.930	6.909	37	$\bar{1}11$
4.920	4.916	59	111
4.630	4.642	9	$\bar{1}31$
4.490	4.493	13	$\bar{2}01$
4.340	4.355	22	$\bar{1}12$
4.013	4.010	9	$\bar{2}21$
3.917	3.925	5	041
3.878	3.868	68	131
3.818	3.815	5	003
3.749	3.750	5	$\bar{2}02$
3.541	3.577	5	$\bar{1}32$
3.446	3.454	100	$\bar{2}22$
3.332	3.326	14	201
3.270	3.270	22	$\bar{1}30$
3.214	3.206	54	$\bar{1}51$
3.063	3.059	9	240
	3.059		042
2.958	2.982	10	$\bar{1}13$
	2.982		311
	2.955		060
2.920	2.914	39	151
	2.899		132
2.860	2.879	33	$\bar{2}03$
	2.863		$\bar{2}42$
	2.842		$\bar{3}12$
2.793 Å	2.818 Å	9	003
	2.789		061
	2.783		$\bar{1}52$
	2.783		310
2.690	2.693	18	$\bar{3}31$
	2.693		133
	2.686		023
2.554	2.588	16	$\bar{3}32$
	2.558		202
	2.544		330
2.460	2.476	7	$\bar{3}13$
	2.469		$\bar{2}61$
	2.458		222
2.425	2.425	16	170
	2.425		152
	2.422		260
	2.422		062
	2.414		243
2.226	2.216	7	080
	2.216		242
2.193	2.209	4	261
	2.206		350
	2.206		172
	2.183		421
	2.178		$\bar{4}22$
	2.178		224
2.095	2.113 Å	5	400
	2.113		004
	2.105		$\bar{1}34$
	2.098		$\bar{4}03$
	2.083		$\bar{3}14$
2.052	2.062	6	$\bar{2}63$
	2.056		420
	2.056		024
	2.043		353
	2.041		423
	2.039		063
2.000	2.015	9	172
	2.015		312
	2.008		441
	2.004		442
	2.004		$\bar{2}44$
	2.000		351
	2.000		153
	1.988		$\bar{2}81$
1.961	1.977	3	223
	1.977		$\bar{3}34$
	1.963		280
	1.963		082
1.942	1.942	5	$\bar{3}71$
	1.942		$\bar{1}73$
	1.934		262
1.910 Å	1.919 Å	9	190
	1.918		332
	1.908		$\bar{2}82$
	1.908		$\bar{1}91$
	1.905		044
	1.905		440
	1.902		$\bar{3}72$
	1.902		$\bar{4}43$
1.872	1.884	9	114
	1.875		$\bar{4}04$
1.839	1.852	4	421
	1.844		281
	1.844		243
	1.838		191
	1.835		$\bar{4}24$
1.776	1.792	17	$\bar{4}61$
	1.788		$\bar{4}62$
	1.788		$\bar{2}64$
	1.779		373
	1.779		$\bar{5}11$
	1.779		$\bar{1}15$
	1.777		$\bar{2}25$
	1.773		0 10 0
	1.760		352

Determination of the structure

STRUNZ and TENNYSON (1956) give the following unit-cell parameters for epistilbite collected at Berufjord, Iceland:

Monoclinic, $a = 8.92$ Å, $b = 17.73$ Å, $c = 10.21$ Å, β(morph) $= 124°20'$.

The crystal sample used in our study, also from Berufjord, Iceland, has a monoclinic unit cell with $a = 9.05 \pm .01$ Å, $b = 17.77 \pm .01$ Å, $c = 10.20 \pm .01$ Å, $\beta = 124°20'$. Differences in relative amounts of substituting sodium may explain the difference in the a-axis lengths between the STRUNZ and TENNYSON cell and ours.

Examination of preliminary Weissenberg and precession photographs suggested an alternate possibility: monoclinic, $a = 9.04$, $b = 17.75$, $c = 9.08$ Å, $\beta = 111°50'$.

This cell was more clearly evident on the Weissenberg photographs. The alternate cell was chosen as more convenient for the purposes of structure analysis and presentation.

The relation between the indices of the alternate cell used in this study and those of the cell reported by PERROTTA (1967) and STRUNZ is given by the following transformation matrix:

$$\begin{pmatrix} 0 & 0 & 0 \\ 0 & 1 & 0 \\ -1 & 0 & 1 \end{pmatrix}.$$

The lattice parameters were refined with the aid of a least-squares refinement program written by E. M. KANE.

Precession and Weissenberg photographs revealed systematic extinctions for $h + k = 2n + 1$ making space groups $C2/m$, Cm and $C2$ possible choices. BOND (1942) presented evidence placing epistilbite from the same locality as our specimen in a non-centric space group, reducing the possibilities to Cm and $C2$. The zero-moment test for centricity (HOWELLS, PHILLIPS and RODGERS, 1950) is illustrated in Fig. 2. The results of this test are not clearcut. Either a centrosymmetric unit cell or a non-centric cell which closely approaches centro-

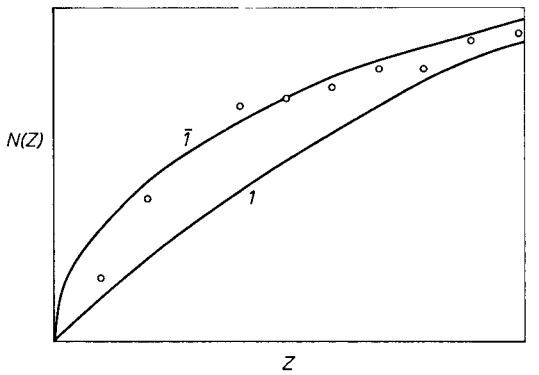

Fig. 2. The zero-moment test for centricity

symmetry are permissible interpretations. In light of the behavior of the structure refinement, the latter interpretation seems correct, the space group is determined as $C2$.

The trial structure was deduced from consideration of the three-dimensional Patterson and comparison with previously determined structures. The Patterson function gave direct information on the position of Si(1), O(2) and O(5) (Table 2). The remaining atoms of the framework were suggested by the Patterson function and by analogy with known zeolite structures. The trial structure assumed fifteen independent atoms in space group $C2/m$. Water molecule positions were determined from three-dimensional Fourier maps.

The initial shifting of the atomic coordinates of the trial structure was carried out using the method of differential Fourier synthesis. An IBM 1710 computer performed the computations with the programs of SLAUGHTER (1964). Scattering factors for neutral atoms were employed and the scattering factors for silicon were used for all

Table 2. *Atomic parameters of epistilbite*

Atom	x	y	z	σ_x	σ_y	σ_z	B	Occupancy		Symmetry
Si,Al(1)	.342	.089	.337	.004 Å	.004 Å	.005 Å	0.75	Si	—.75	
								Al	—.25	
Si,Al(2)	.405	.209	.111	.005	.005	.005	1.68	Si	—.85	
								Al	—.15	
Si,Al(3)	.610	.303	.401	.005	.005	.006	1.78	Si	—.60	
								Al	—.40	
O(1)	.304	.000	.285	.012	—	.021	1.68			$C2/m$
O(2)	.500	.098	.500	—	.022	—	2.78			
O(3)	.000	.176	.500	—	.021	—	3.08			
O(4)	.500	.182	.000	—	.017	—	2.38			
O(5)	.182	.115	.370	.018	.015	.016	1.80			
O(6)	.358	.137	.187	.013	.013	.018	1.90			
O(7)	.467	.281	.207	.018	.014	.022	3.10			
O(8)	.449	.755	.733	.016	.014	.022	2.50			
O(9)	.217	.227	.964	.016	.014	.023	1.85			$C2$
O(10)	.277	.238	.561	.017	.020	.020	2.60			
Ca(1)	.990	.000	.750	.008	—	.009	2.50	Ca	—.58	
Ca(2),HOH	.247	.000	.003	.026	—	.034	2.78	Ca	—.16	$C2/m$
								HOH	—.13	
HOH(1)	.799	.084	.191	.021	.020	.028	5.0_0		1.0	
HOH(2)	.771	.916	.231	.027	.020	.027	4.6_5		1.0	$C2$
HOH(3)	.000	.000	.500	—	—	—	4.4_0		1.0	
HOH(4)	.500	.000	.000	—	—	—	4.6_0		0.50	
HOH(5)	.000	.079	.000	—	.050	—	4.5_0		0.70	$C2/m$
HOH(6)	.000	.000	.000	—	—	—	4.2_0		0.30	

Centrosymmetric atoms 15
Noncentrosymmetric 6
Total HOH per cell 14.9

Si—Al positions until final stages of refinement. Solution of the structure employed 822 reflections observed by photographic methods. With new data, collected by counter methods, refinement was reinitiated in space group $C2/m$ as before. Refinement stopped in the centrosymmetric space group at $R = 0.23$ for the disordered structure with $R = \frac{\Sigma||F_o| - |F_c||}{\Sigma|F_o|}$. In space group $C2/m$ all oxygen atoms on or near $y = 0.25$ had temperature factors larger than 7.5 and Si—O

Table 3. *Interatomic distances in epistilbite*

Si,Al(1)—O(1)		1.64 Å	Si,Al(3)′—O(3)	*	1.62 Å
O(2)		1.64	O(5)		1.66
O(5)		1.64	O(8)		1.54
O(6)		1.66	O(10)		1.82
	Mean	1.64		Mean	1.66
Si,Al(2)—O(4)		1.62	Si,Al(1)—Si,Al(1)		3.26
O(6)		1.60	Si,Al(2)		3.14
O(7)		1.52	Si,Al(2)		3.17
O(9)		1.77	Si,Al(3)		3.04
	Mean	1.62		Mean	3.16
Si,Al(3)—O(3)		1.62	Si,Al(2)—Si,Al(1)		3.17
O(5)		1.66	Si,Al(2)		3.09
O(7)		1.81	Si,Al(2)		3.14
O(10)		1.50	Si,Al(3)		3.10
	Mean	1.65		Mean	3.13
Si,Al(2)′—O(4)	*	1.62	Si,Al(3)—Si,Al(1)		3.04
O(6)		1.60	Si,Al(2)		3.10
O(8)		1.69	Si,Al(3)		3.15
O(9)		1.55	Si,Al(3)		3.14
	Mean	1.61		Mean	3.11
Ca(1)—O(1)		2.56 (1)	Ca(2)—O(1)		2.42 Å (1)
O(5)		2.55 (2)	O(6)		2.90 (2)
HOH(1)		2.57 (1)	HOH(1)		2.23 (1)
HOH(2)		2.32 (1)	HOH(2)		2.55 (1)
HOH(3)		2.32 (1)	HOH(4)		2.32 (1)
HOH(5)		2.65 (2)	HOH(5)		2.62 (2)
Ca(1)—Ca(1)		4.63	Ca(2)—Ca(2)		4.44
		4,50			4.60

* Prime indicates the mirror equivalent of the unprimed atom. Numbers in parenthesis to right of distance give numbers of equivalent distances.

Table 4. *Observed and calculated structure factors of disordered epistilbite*

h	k	l	F_o	F_c
2	0	0	44.1	38.9
4			19.5	15.6
6			62.6	53.9
8			37.3	43.4
1	1	0	6.8	5.7
3			87.0	88.0
5			24.6	30.9
7			26.7	28.9
9			45.1	41.3
0	2	0	111.0	111.3
2			62.6	63.9
4			77.4	86.1
6			111.3	111.6
8			21.9	15.1
1	3	0	32.5	31.1
3			57.6	58.0
5			11.3	9.4
7			20.3	23.7
9			13.5	4.1
0	4	0	43.1	37.9
2			87.1	86.9
4			73.6	73.5
6			86.2	90.6
1	5	0	85.5	86.2
3			14.9	11.9
5			13.7	12.9
7			89.5	95.6
9			12.2	9.4
0	6	0	75.1	68.2
4			34.7	22.4
6			34.5	26.1
8			48.2	37.4
1	7	0	23.7	39.0
3			16.1	26.8
7			29.8	16.4
9			16.9	23.3
0	8	0	17.8	19.6
2			68.8	60.2
6			41.6	41.1
8			33.9	25.6
1	9	0	18.2	16.2
3			33.1	30.7
5			46.8	46.8
7			17.9	9.6
0	10	0	205.9	224.3
2			52.0	47.9
4			54.5	49.0
6			23.6	19.6
8			28.0	24.6
1	11	0	18.4	28.5
3			41.2	38.5
5			44.7	47.0
7			17.3	18.9
0	12	0	27.2	39.0
2			21.7	32.0
4			90.0	88.0
6			79.3	86.0
8			7.2	5.2
1	13	0	25.9	22.2
3			90.8	93.8
7			12.4	11.8
0	14	0	76.9	67.2
2			16.3	20.3
4			25.4	26.7
6			18.6	21.7
1	15	0	30.8	31.5
0	16	0	13.0	5.5
2			17.3	21.6
4			34.5	32.1
6			21.4	10.9
1	17	0	55.6	55.8
3			35.7	35.0
5			7.4	6.2
0	18	0	52.7	47.3
2			19.9	16.8
4			72.3	64.2
1	19	0	9.8	5.3
2	20	0	21.7	13.5
0	0	1	52.3	57.5
2			124.7	133.6
4			22.6	27.0
6			67.4	67.4
8			17.9	18.4
1	1	1	146.3	138.6
3			52.3	85.8
5			97.1	99.9
7			51.3	24.7
9			45.6	29.9
0	2	1	16.8	30.8
2			19.8	21.7
4			37.3	40.5
6			30.0	16.8
8			24.6	32.6
1	3	1	206.2	194.1
5			89.4	89.5
7			47.1	44.0
9			16.9	24.1
0	4	1	87.2	78.7
2			50.8	51.8
4			8.0	7.5
6	4	1	38.8	35.7
8			36.8	46.8
1	5	1	167.3	182.4
3			65.9	70.8
5			17.1	5.7
7			25.0	39.6
9			8.5	6.1
0	6	1	25.6	31.1
2			69.6	76.3
4			32.2	29.4
6			54.7	50.1
8			32.0	32.6
3	7	1	74.2	75.3
5			119.5	124.1
7			53.8	61.8
0	8	1	15.5	7.6
2			12.0	18.0
4			42.8	42.4
6			31.4	37.7
8			7.9	11.3
1	9	1	75.9	67.3
5			67.1	72.3
7			16.7	14.3
0	10	1	45.7	45.1
2			43.3	37.9
4			32.8	21.6
6			26.0	26.6
8			9.3	6.0
1	11	1	39.4	35.3
3			60.4	49.5
5			29.4	21.5
0	12	1	35.2	39.0
2			24.3	15.5
4			50.7	50.5
6			12.0	13.5
1	13	1	86.2	76.2
3			45.2	31.7
5			19.8	14.3
7			25.5	24.0
0	14	1	67.2	64.1
2			68.7	59.7
4			17.9	14.0
6			12.8	16.0
1	15	1	100.0	86.8
5			16.7	18.2
0	16	1	22.2	13.5
2			69.5	66.9
4			16.2	15.4
1	17	1	50.4	44.2
3			38.1	37.4
5			74.5	73.7
0	18	1	39.9	36.2
2			16.5	22.3
4			13.5	10.5
1	19	1	33.3	22.4
3			24.9	12.8
0	20	1	28.4	19.9
2			14.1	7.2
0	0	2	14.4	13.2
2			214.9	214.0
4			115.5	110.5
8			29.8	53.9
1	1	2	106.0	103.0
3			80.9	85.6
5			54.7	61.2
7			40.4	40.8
0	2	2	104.0	105.8
2			96.5	97.5
4			28.8	32.2
6			12.8	24.6
8			14.9	17.5
1	3	2	40.8	39.7
3			11.4	11.6
5			17.1	26.3
7			25.6	25.6
0	4	2	57.4	39.5
2			80.1	78.3
6			38.3	34.6
8			18.9	6.9
1	5	2	122.0	107.7
3			25.7	15.5
5			30.8	26.0
7			50.0	63.4
0	6	2	48.6	55.6
2			64.5	60.0
6			48.5	44.1
8			30.6	30.2
1	7	2	52.8	48.9
3			17.9	15.7
5			42.6	49.7
7			38.1	39.3
0	8	2	91.2	87.2
2			95.0	98.0
4			48.1	49.3
6			17.7	12.3
8			20.7	30.3
1	9	2	22.6	16.1
3			77.0	84.7
5			29.2	27.8
7			16.0	26.7
0	10	2	27.8	29.8
2			92.0	87.7
4			35.8	49.3
6			34.9	30.2
1	11	2	80.2	86.4
3			8.1	8.0
5			53.2	63.3
7			10.8	6.6
0	12	2	37.9	44.7
2			103.1	113.7
4			36.8	31.3
6			22.6	33.8
1	13	2	11.2	20.3
3			31.6	37.4
5			10.6	7.8
0	14	2	37.9	37.8
2			22.6	20.2
4			29.2	15.9
6			31.7	45.6
1	15	2	7.8	19.9
3			17.5	15.6
5			17.6	5.7
0	16	2	6.7	15.3
2			27.4	25.9
4			50.4	43.6
1	17	2	29.3	31.0
3			16.6	16.9
0	18	2	7.1	14.1
2			18.6	18.6
1	19	2	43.7	41.8
0	20	2	3.6	9.0
0	0	3	45.6	45.4
2			96.8	103.4
4			28.5	32.5
6			51.6	62.9
8			8.2	14.6
1	1	3	51.9	82.7
3			28.1	14.7
7			22.1	6.0
0	2	3	77.1	69.3
2			31.2	23.1
4			31.6	20.8
6			7.6	11.4
8			18.5	11.8
1	3	3	44.9	63.3
3			125.4	135.9
5			51.6	38.4
7			16.0	17.6
0	4	3	12.0	21.8
2			38.1	37.3
4			52.5	42.3
6			18.9	17.4
8			25.9	12.1
1	5	3	55.7	50.8
3			190.3	210.8
5			46.5	49.5
7			46.1	64.4
0	6	3	49.0	47.8
2			44.1	22.0
4			59.7	43.2
6			36.1	32.2
1	7	3	75.6	79.7
3			6.5	25.0
5			15.6	28.4
7			28.4	6.8
0	8	3	16.6	11.3
2			27.9	20.0
4			47.9	52.2
6			33.6	31.9
3	9	3	47.7	40.5
5			34.7	12.5
7			18.7	6.4
0	10	3	57.7	64.1
2			67.2	65.4
4			22.2	20.3
6			33.0	43.3
1	11	3	87.8	80.4
3			81.6	75.3
0	12	3	77.2	72.0
2			5.9	5.5
4			43.6	43.5
6			24.7	16.0
1	13	3	34.4	16.9
3			68.0	69.7
5			23.1	6.2
0	14	3	40.1	26.4
2			16.2	13.6
4			29.7	36.1
1	15	3	8.7	6.8
3			62.0	64.1
5			22.9	21.4
0	16	3	6.7	5.8
2			20.9	15.2
4			34.8	25.2
1	17	3	35.8	29.4
3			28.2	19.6
0	18	3	30.3	24.9
2			11.6	11.4
1	19	3	16.7	4.5
0	0	4	8.8	14.1
2	0	4	133.4	129.6
4			124.3	139.2
6			7.9	11.4
1	1	4	17.0	15.0
3			32.3	29.3
5			35.3	25.8
7			8.9	8.0
0	2	4	87.4	97.0
2			44.6	17.4
6			31.6	27.2
1	3	4	20.0	17.5
3			17.8	3.7
5			35.9	34.6
7			27.0	32.1
0	4	4	79.8	71.3
4			6.5	19.6
6			59.2	44.5
1	5	4	67.6	75.0
3			55.3	57.9
5			36.9	31.1
7			9.0	14.4
0	6	4	54.6	49.9
4			29.3	45.2
6			65.2	59.8
1	7	4	16.6	24.7
3			68.5	65.2
5			24.2	15.7
7			24.5	30.0
0	8	4	77.4	82.2
2			48.0	31.5
4			25.8	44.2
6			27.5	8.5
1	9	4	15.6	9.8
3			8.6	7.0
5			18.3	17.2
0	10	4	64.9	67.9
2			88.4	91.2
4			68.3	80.5
6			7.5	4.8
1	11	4	47.7	48.9
3			14.9	5.2
5			57.5	66.6
0	12	4	103.8	103.3
2			64.0	58.2
4			20.7	37.9
1	13	4	16.9	13.0
3			21.6	30.3
5			35.5	27.3
0	14	4	18.0	16.3
2			27.8	19.6
4			28.4	29.2
1	15	4	39.3	31.7
3			52.1	49.0
0	16	4	42.1	41.3
2			30.5	14.1
1	17	4	16.1	3.7
0	18	4	48.9	43.5
0	0	5	36.1	41.6
2			89.5	89.1
4			21.3	1.2
6			19.2	22.6
1	1	5	93.4	98.5
5			30.8	39.7
0	2	5	13.2	20.9
2			14.2	10.5
4			17.7	28.7
6			24.4	21.9
1	3	5	75.5	86.2
3			47.5	33.0
5			41.4	57.8
0	4	5	36.4	33.1
2			26.5	21.0
4			15.2	9.0
6			21.0	7.9
1	5	5	19.9	12.7
3			33.2	35.0
0	6	5	35.7	27.5
2			57.5	55.4
4			53.3	58.4
6			14.8	6.0
1	7	5	144.5	149.3
3			14.5	26.9
0	8	5	10.6	8.0
2			5.1	7.6
4			23.8	17.1
6			7.2	3.3
1	9	5	85.1	96.8
3			28.0	17.8
5			13.7	14.4
0	10	5	21.9	12.6
2			30.6	28.9
4			19.0	13.6
1	11	5	34.1	29.0
3			47.0	40.2
5			25.5	37.4
0	12	5	17.0	22.2
2			28.1	21.8
4			35.4	40.2
1	13	5	14.1	6.6
3			22.8	7.8

Table 4. *(Continued)*

h	k	l	F_o	F_c	h	k	l	F_o	F_c	h	k	l	F_o	F_c	h	k	l	F_o	F_c
0	14	5	15.6	15.7	-2	4	1	29.3	42.6	-3	9	2	26.0	25.0	-1	15	3	76.8	64.5
2			16.3	15.3	-4			8.7	7.0	-5			23.1	21.9	-3			10.2	10.5
1	15	5	7.1	5.9	-6			13.3	13.8	-7			57.8	59.8	-5			34.4	27.1
3			7.4	4.9	-8			35.6	32.3	-9			24.2	25.0	-7			38.6	25.6
0	16	5	45.0	47.4	-10			15.7	9.0	-2	10	2	3.9	5.9	-2	16	3	68.6	65.3
2			33.6	34.5	-1	5	1	177.6	178.0	-4			88.8	86.5	-4			24.5	23.5
1	17	5	66.0	67.5	-3			23.7	5.0	-6			8.2	3.4	-6			66.8	57.3
0	18	5	19.2	18.4	-5			122.0	121.3	-8			79.1	86.6	-1	17	3	61.5	45.3
0	0	6	36.5	25.6	-9			58.5	67.3	-1	11	2	89.4	96.2	-3			100.4	86.9
4			23.6	10.9	-2	6	1	16.7	18.3	-3			81.5	74.7	-5			20.1	21.5
1	1	6	58.1	56.9	-4			21.9	31.8	-5			42.6	44.4	-2	18	3	42.7	34.5
3			28.0	27.4	-6			14.7	15.1	-7			12.7	4.4	-1	19	3	39.8	33.7
0	2	6	81.5	74.6	-8			35.2	28.5	-2	12	2	162.9	152.9	-3			15.5	13.5
1	3	6	28.9	32.3	-1	7	1	21.3	21.0	-4			38.4	36.8	-4	0	4	273.1	272.1
3			36.9	38.8	-3			79.5	75.1	-6			56.1	49.2	-6			88.8	92.9
0	4	6	98.7	101.5	-5			72.6	71.1	-8			12.5	11.7	-8			33.3	41.6
2			42.2	36.5	-7			25.1	8.7	-3	13	2	14.9	18.1	-3	1	4	20.8	17.4
1	5	6	55.6	46.2	-9			35.1	46.9	-5			12.2	14.9	-5			9.6	9.2
3			37.0	30.3	-2	8	1	12.6	14.9	-7			31.2	29.8	-7			59.6	65.7
0	6	6	69.2	56.9	-4			37.3	38.4	-2	14	2	54.1	48.1	-9			10.7	8.5
2			39.1	15.5	-6			28.7	23.2	-4			65.3	59.9	-2	2	4	47.1	56.8
1	7	6	19.7	17.0	-8			38.4	36.2	-6			23.5	14.3	-4			24.2	17.3
3			59.2	58.8	-1	9	1	60.4	59.5	-1	15	2	22.3	22.5	-6			76.4	68.7
0	8	6	26.0	12.4	-5			37.2	24.4	-3			9.8	12.1	-8			25.1	20.8
2			11.0	15.3	-7			33.2	20.4	-5			23.1	21.9	-10			65.1	70.3
1	9	6	12.3	8.1	-9			9.7	15.3	-7			19.1	14.9	-3	3	4	27.1	31.0
0	10	6	15.0	7.5	-2	10	1	28.4	25.0	-4	16	2	23.0	23.8	-5			12.2	13.3
1	11	6	49.2	53.0	-4			48.6	53.5	-6			34.2	24.4	-7			19.7	37.6
0	12	6	63.5	67.0	-6			59.0	61.1	-1	17	2	13.3	14.0	-9			26.6	22.5
0	0	7	27.6	23.5	-8			25.8	22.2	-3			13.1	3.2	-2	4	4	80.0	77.3
4			9.4	26.4	-1	11	1	39.4	32.8	-5			42.1	35.4	-4			56.6	68.0
3	1	7	25.4	5.4	-3			28.8	28.2	-2	18	2	17.0	22.9	-6			61.6	66.3
2	2	7	20.2	12.2	-5			32.3	28.3	-4			26.0	22.5	-8			27.3	23.9
4			15.9	17.6	-7			50.9	47.3	-1	19	2	5.6	2.7	-10			37.8	39.1
3	3	7	16.3	18.3	-2	12	1	37.3	37.8	-3			30.3	26.9	-3	5	4	58.4	63.7
2	4	7	67.9	63.6	-4			103.2	101.0	-2	20	2	35.9	29.5	-5			66.6	71.9
4			17.0	7.7	-6			15.0	7.6	-2	0	3	30.6	29.0	-7			28.0	38.1
3	5	7	45.0	62.6	-8			17.4	20.0	-4			95.5	108.7	-9			7.4	4.4
2	6	7	51.2	36.8	-1	13	1	53.0	47.0	-6			49.4	53.9	-2	6	4	32.5	42.9
4			12.2	12.4	-3			72.4	60.5	-8			21.4	19.7	-4			27.2	25.1
1	7	7	36.9	44.6	-5			26.5	23.6	-10			13.1	11.1	-6			56.9	54.3
3			14.8	19.1	-7			36.0	30.6	-3	1	3	39.4	48.2	-8			48.9	41.8
0	8	7	8.1	7.2	-2	14	1	52.0	54.4	-5			51.1	54.0	-10			21.2	22.4
2			21.8	16.4	-4			12.5	10.9	-7			49.7	48.6	-1	7	4	37.2	71.0
1	9	7	19.5	20.9	-6			20.7	17.1	-9			37.1	21.3	-3			39.2	46.4
3			33.4	25.0	-1	15	1	37.8	28.1	-2	2	3	16.7	9.1	-5			31.3	39.2
0	10	7	25.1	13.7	-3			81.8	70.1	-4			19.2	27.1	-7			9.7	8.8
2			7.0	23.5	-5			51.1	43.6	-6			38.3	39.1	-9			9.2	6.3
1	11	7	26.7	9.7	-7			34.0	28.1	-8			24.9	30.4	-2	8	4	88.0	87.3
0	12	7	22.5	15.5	-2	16	1	61.8	52.9	-10			37.9	40.2	-4			18.2	18.3
2			34.0	26.7	-4			19.6	16.6	-3	3	3	10.8	21.4	-6			91.4	88.6
1	13	7	24.3	25.9	-6			27.6	25.0	-5			47.3	37.3	-8			32.8	32.2
0	14	7	10.2	10.1	-1	17	1	33.3	33.9	-7			62.0	59.4	-3	9	4	30.6	32.2
0	0	8	46.6	53.1	-3			61.4	47.7	-9			21.9	11.0	-5			35.3	32.2
2			26.1	38.2	-5			23.2	15.9	-2	4	3	51.5	53.9	-7			11.5	9.8
1	1	8	38.4	40.6	-2	18	1	18.4	13.0	-4			18.2	20.3	-9			14.2	13.2
3			16.9	9.5	-4			72.2	63.1	-6			34.1	35.8	-2	10	4	75.6	74.4
0	2	8	32.1	15.7	-1	19	1	12.5	9.9	-8			18.9	25.4	-4			121.0	124.6
2			21.3	23.2	-3			31.9	25.6	-10			22.2	19.1	-6			89.9	90.7
1	3	8	25.4	13.1	-2	0	2	104.0	96.7	-1	5	3	35.2	36.6	-8			5.6	3.7
3			29.2	32.8	-4			18.7	8.8	-3			27.9	28.3	-1	11	4	82.6	56.4
0	4	8	49.6	28.6	-6			25.5	10.4	-5			88.5	88.1	-3			26.0	20.5
2			34.6	20.1	-10			8.9	14.2	-7			97.5	97.2	-5			10.7	17.0
1	5	8	52.1	56.9	-1	1	2	110.0	110.0	-9			34.2	36.7	-7			65.9	67.7
3			24.2	17.1	-3			65.8	59.7	-2	6	3	47.7	44.9	-9			14.3	16.9
0	6	8	21.6	29.3	-5			29.3	35.8	-4			71.1	78.7	-2	12	4	33.1	31.7
2			36.6	30.9	-7			30.7	31.1	-6			84.1	88.0	-4			55.0	65.0
1	7	8	20.5	7.3	-9			33.9	33.6	-10			33.7	33.6	-6			48.6	47.4
0	8	8	22.9	11.7	-4	2	2	35.7	40.1	-1	7	3	82.4	84.9	-8			29.2	27.8
2			35.0	38.7	-6			66.8	60.2	-3			157.0	168.4	-3	13	4	6.6	9.8
1	9	8	12.7	13.0	-8			56.9	52.0	-5			35.3	35.6	-5			14.1	10.8
0	10	8	43.0	46.2	-10			27.0	25.0	-7			92.0	88.5	-7			17.4	28.7
0	12	8	20.6	16.3	-1	3	2	18.2	25.1	-9			39.2	37.7	-2	14	4	34.4	36.6
0	0	9	44.5	35.8	-3			9.0	18.5	-2	8	3	43.7	40.2	-4			24.9	25.6
1	1	9	29.4	30.3	-5			9.3	16.7	-4			14.2	12.9	-6			37.0	29.2
0	2	9	9.1	7.6	-7			25.7	27.3	-6			6.1	13.1	-1	15	4	40.0	25.8
1	3	9	20.9	26.8	-2	4	2	147.5	164.2	-8			22.3	24.1	-3			25.7	23.4
0	4	9	13.6	6.3	-4			105.6	107.1	-1	9	3	46.1	45.2	-5			42.8	37.4
1	5	9	6.7	3.7	-8			12.8	17.9	-3			53.7	59.2	-7			4.3	4.6
0	6	9	27.8	46.3	-10			8.6	17.6	-5			11.4	8.8	-2	16	4	35.3	36.9
-2	0	1	90.0	93.8	-1	5	2	41.3	48.4	-7			32.3	32.4	-4			21.8	18.2
-4			98.9	104.5	-3			39.8	37.3	-4	10	3	58.2	55.6	-6			9.2	8.0
-6			45.2	47.6	-5			34.4	33.2	-6			39.0	45.2	-1	17	4	33.7	43.1
-8			34.2	31.1	-7			10.7	8.7	-8			12.3	11.0	-3			36.7	38.5
-10			28.5	34.0	-9			11.6	7.1	-1	11	3	25.3	28.2	-5			28.6	29.0
-1	1	1	86.4	95.2	-2	6	2	49.2	56.8	-3			75.5	70.8	-2	18	4	43.5	31.2
-3			58.0	59.0	-4			25.5	30.4	-5			50.9	48.8	-4			20.5	21.3
-5			34.7	66.8	-6			63.5	62.3	-7			60.5	56.1	-1	19	4	39.8	25.1
-7			61.3	44.9	-8			40.4	42.4	-9			38.5	30.9	-3			35.5	27.9
-9			14.1	20.4	-10			34.2	14.2	-2	12	3	14.0	11.5	-4	0	5	4.7	15.2
-2	2	1	55.4	64.0	-1	7	2	47.1	49.3	-4			40.4	42.3	-6			33.3	31.3
-4			74.3	74.6	-3			23.1	24.8	-6			24.9	28.0	-10			4.1	9.5
-6			8.6	12.0	-5			62.3	60.8	-8			30.1	33.7	-3	1	5	54.3	53.7
-8			20.9	14.3	-7			14.3	2.4	-1	13	3	97.6	83.0	-5			48.7	66.9
-10			6.3	0.8	-9			36.5	47.2	-3			11.8	22.9	-7			34.3	34.9
-1	3	1	47.0	55.6	-2	8	2	53.4	58.0	-5			13.7	10.2	-9			7.1	5.2
-3			116.2	111.9	-4			87.1	82.3	-7			13.6	10.2	-4	2	5	13.5	16.3
-5			13.0	20.0	-6			68.6	66.8	-2	14	3	34.7	31.0	-6			40.5	44.0
-7			48.7	52.0	-8			59.6	63.7	-4			5.1	14.7	-8			14.5	19.9
-9			33.6	42.8	-1	9	2	63.5	63.3	-6			17.3	19.0	-10			5.2	10.8

Table 4. *(Continued)*

h	k	l	F_o	F_c	h	k	l	F_o	F_c	h	k	l	F_o	F_c	h	k	l	F_o	F_c
-3	3	5	49.5	50.2	-6	0	6	81.8	81.4	-6	14	6	14.0	10.9	-3	3	8	19.7	18.3
-5			75.0	81.4	-8			65.8	54.7	-1	15	6	12.5	9.8	-7			17.3	16.1
-7			42.4	35.1	-10			68.3	73.6	-3			12.5	14.4	-9			5.3	2.5
-9			36.0	32.9	-3	1	6	50.3	48.6	-5			10.1	7.3	-2	4	8	33.8	34.5
-2	4	5	12.2	13.7	-5			41.8	48.5	-2	16	6	20.7	10.0	-4			34.7	26.9
-4			69.7	70.7	-7			42.3	49.3	-4			4.7	9.8	-6			21.2	14.9
-6			30.4	36.4	-9			17.3	29.2	-1	17	6	43.0	19.7	-8			15.9	8.7
-8			9.3	9.2	-4	2	6	105.4	111.1	-3			42.3	38.4	-3	5	8	45.4	55.3
-10			12.1	10.7	-6			7.5	24.8	-4	0	7	71.4	68.7	-5			30.6	35.6
-3	5	5	56.1	60.9	-8			41.1	36.8	-6			45.2	52.0	-7			30.8	32.3
-5			197.4	192.5	-10			8.0	5.7	-8			37.8	44.2	-6	6	8	8.5	17.0
-7			10.5	9.3	-3	3	6	20.9	27.8	-5	1	7	63.3	58.1	-8			20.6	27.4
-9			74.8	70.9	-5			9.3	12.9	-7			50.7	56.2	-3	7	8	12.0	15.6
-2	6	5	32.9	33.6	-7			10.5	11.6	-9			7.9	7.8	-5			31.1	25.2
-4			15.2	17.0	-4	4	6	48.1	46.5	-4	2	7	15.8	26.1	-7			16.5	16.9
-6			10.2	15.8	-6			75.4	83.3	-8			9.1	15.7	-4	8	8	30.5	29.5
-8			7.9	11.1	-8			26.5	23.5	-3	3	7	73.8	72.6	-6			42.7	43.7
-10			12.8	10.4	-10			10.8	3.6	-5			36.5	23.6	-8			8.6	9.3
-3	7	5	37.2	38.5	-3	5	6	67.2	71.8	-7			52.9	51.9	-1	9	8	35.3	21.4
-5			63.6	55.5	-5			23.0	22.8	-9			32.0	32.1	-3			23.0	21.7
-9			30.5	25.0	-7			7.1	9.2	-4	4	7	28.2	38.6	-5			42.7	42.4
-2	8	5	51.8	45.5	-9			26.3	30.0	-6			10.7	7.9	-7			26.2	19.4
-4			31.8	33.0	-4	6	6	43.9	43.4	-3	5	7	80.4	93.7	-4	10	8	5.1	4.9
-6			11.7	13.3	-6			29.6	38.7	-5			8.4	11.8	-6			58.7	52.3
-8			15.7	14.0	-8			13.0	10.8	-7			21.6	12.6	-1	11	8	31.5	10.3
-3	9	5	22.0	19.0	-3	7	6	12.9	30.8	-9			16.7	14.5	-3			2.9	6.3
-5			15.1	16.0	-5			17.9	18.4	-2	6	7	2.9	7.9	-5			28.9	33.0
-7			10.0	14.5	-7			8.6	13.0	-4			49.2	57.5	-2	12	8	15.3	15.9
-9			24.0	23.9	-9			33.2	35.5	-6			38.3	44.8	-4			10.8	3.9
-2	10	5	36.6	30.3	-4	8	6	96.5	102.8	-8			29.6	30.5	-6			41.4	28.8
-6			36.5	38.9	-6			16.3	19.5	-3	7	7	82.6	83.6	-1	13	8	35.7	13.4
-8			37.9	38.6	-8			39.7	36.7	-7			81.6	91.0	-3			12.1	7.8
-3	11	5	66.5	68.6	-1	9	6	21.9	22.0	-4	8	7	17.6	20.8	-5			38.7	32.1
-7			4.5	5.8	-3			37.1	34.1	-6			24.9	31.0	-6	0	9	21.5	32.3
-2	12	5	48.1	42.9	-5			41.6	43.8	-8			18.1	14.4	-8			7.1	12.8
-4			21.6	18.3	-7			11.8	15.9	-3	9	7	13.3	15.0	-5	1	9	15.3	14.3
-6			41.1	44.2	-9			20.6	17.9	-5			25.7	27.0	-7			13.7	14.9
-8			39.6	44.5	-2	10	6	38.4	40.2	-7			42.6	43.1	-6	2	9	23.9	20.2
-3	13	5	22.3	21.7	-4			54.7	47.0	-4	10	7	26.3	27.9	-8			7.6	8.8
-5			67.9	63.6	-6			32.7	38.7	-3	11	7	39.6	38.0	-5	3	9	36.6	28.7
-7			9.3	5.9	-8			63.0	60.5	-5			23.6	22.2	-7			33.3	28.4
-2	14	5	19.8	17.5	-1	11	6	52.5	49.2	-7			27.8	33.0	-4	4	9	19.4	28.6
-4			31.7	25.2	-3			59.6	55.7	-4	12	7	21.8	23.4	-6			32.9	23.7
-6			20.7	10.6	-5			5.9	5.8	-6			9.2	10.7	-3	5	9	28.9	27.6
-1	15	5	33.6	30.8	-7			45.4	45.4	-3	13	7	22.1	26.5	-7			38.2	31.1
-3			27.2	24.2	-2	12	6	58.4	53.3	-5			14.1	21.1	-4	6	9	24.0	25.1
-5			65.2	51.4	-4			71.4	67.6	-4	14	7	24.6	21.5	-6			21.9	27.9
-2	16	5	29.6	30.4	-6			19.5	26.7	-6	0	8	41.2	67.2	-5	7	9	28.7	26.1
-4			15.6	7.4	-8			48.3	39.6	-8			6.8	29.1	-7			14.9	16.3
-6			32.2	11.1	-1	13	6	12.3	26.0	-5	1	8	57.1	60.3	-4	8	9	6.9	6.3
-1	17	5	27.3	20.2	-3			7.9	14.7	-7			6.2	4.0	-6			33.9	26.1
-3			30.7	27.6	-5			24.9	19.3	-9			19.4	19.8	-5	9	9	30.4	23.7
-5			16.7	11.3	-7			18.3	23.7	-4	2	8	16.9	5.7	-4	10	9	22.9	25.2
-2	18	5	45.1	44.8	-2	14	6	21.9	11.5	-6			53.5	45.0					
-4	0	6	67.3	59.7	-4			19.9	20.1	-8			51.2	51.2					

bond distances were grossly incorrect. Occupancy factors of the two Ca sites and the position and electron densities of the oxygen atoms at $y = 0.27$ interacted strongly. When the occupancy factors of the calcium atoms were adjusted to match observed and calculated electron densities, curvatures, temperature factors, and positions of the quarter-level oxygen atoms were incorrect. Fourier sections near the quarter level along b suggested the space group $C2$.

Refinement was then begun in $C2$ with both differential Fourier synthesis and with the Oak Ridge least-squares program (BUSING, MARTIN and LEVY, 1962) as modified by Dr. R. SHIONO at the University of Pittsburgh. Calculations were run on the University of Pittsburgh IBM 7090 through the kind assistance of Drs. G. A. JEFFREY and R. SHIONO. Refinement proceeded to a final unweighed $R = 0.15$ with the four oxygen atoms near the $y = 0.25$ level assuming positions in $C2$ while the remainder of the structure remained essentially centrosymmetric.

Not only did all bond distances, temperature factors, and scale factors improve after beginning refinement in $C2$, but differentiation of Si sites became evident, with Al substitution for silicon more pronounced in the sites nearest the calcium site of higher occupancy. Temperature and occupancy factors on the water sites also improved. High-symmetry parameters of most of the structure and structural effects of disordering (not yet fully known) caused appreciable parameter interaction. Interaction was strongest among calciums, and the oxygen positions near the plane $y = 0.25$, and were noted especially during refinement in differential synthesis. Final atomic parameters are presented in Table 2. Interatomic distances are presented in Table 3. Observed and calculated structure factors are listed in Table 4.

Discussion of the structure

The framework

The structures of mordenite (MEIER, 1961) and dachiardite (GOTTARDI and MEIER, 1963) were found to be based upon columns of five-membered rings. Epistilbite has a structure which is a variant of the same motif. KERR (1964) suggested a framework for epistilbite which has been found to be essentially correct. KERR's suggested framework (Fig. 3) was developed independently in the course of this study.

The basic structural unit or building block in the framework of epistilbite consists of eight tetrahedra linked to form a central cavity bounded by four pentagonal and four triangular faces. These units

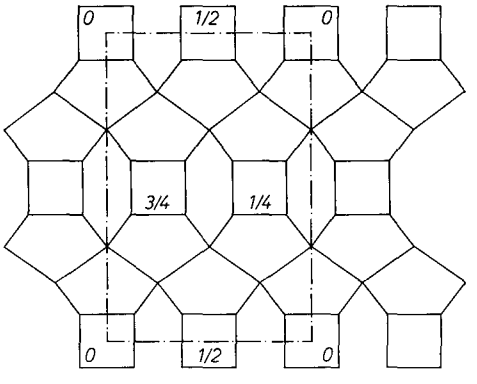

Fig. 3. Projection of the epistilbite structure. Intersections of lines represent silicon positions. Oxygen positions are on the lines between intersections

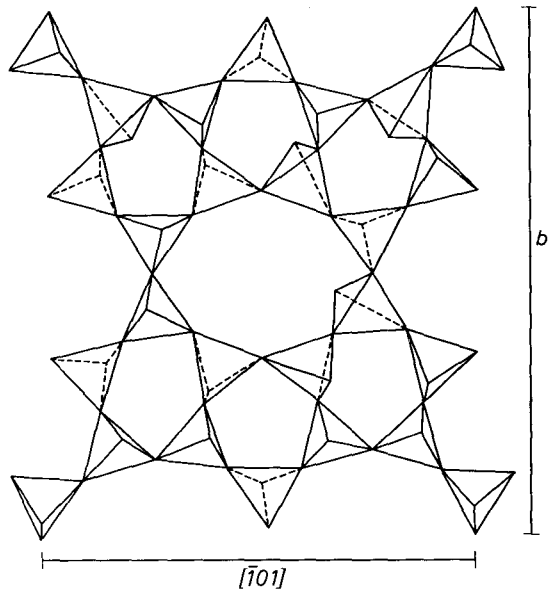

Fig. 4. View of epistilbite structure showing continuous eight-membered-ring channels and five-membered-ring elements of the framework. The b axis is vertical

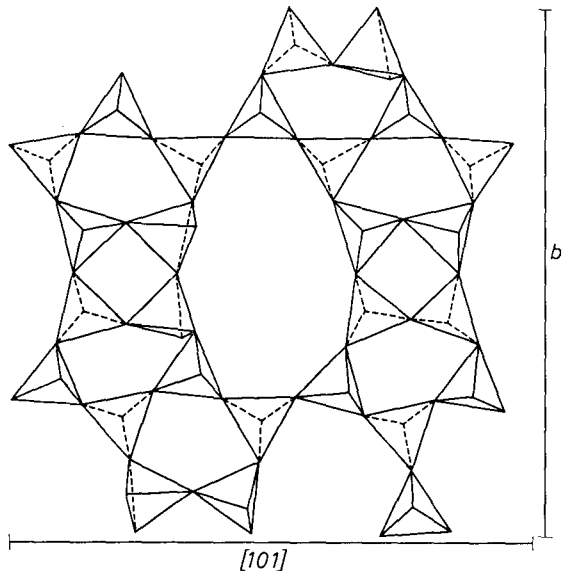

Fig. 5. View showing narrow ten-membered-ring channels blocked in front and behind by four-membered rings. The b axis is vertical; projection is at right angles to that of Fig. 4

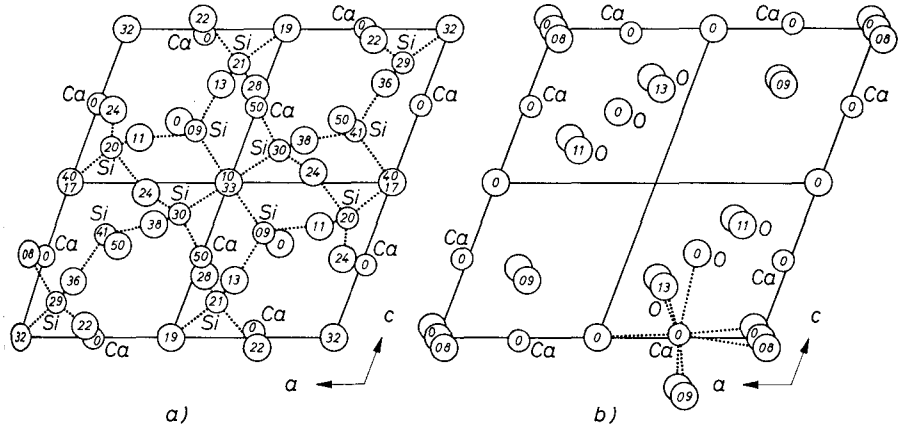

Fig. 6*a*. Projection of framework and calcium atoms in cell from $y = 0$ to $y = 0.5$. Numbers in circles are approximate y coordinates

Fig. 6*b*. Projection of calcium ions, water molecules, and framework oxygen atoms immediately above and below the plane $y = 0$

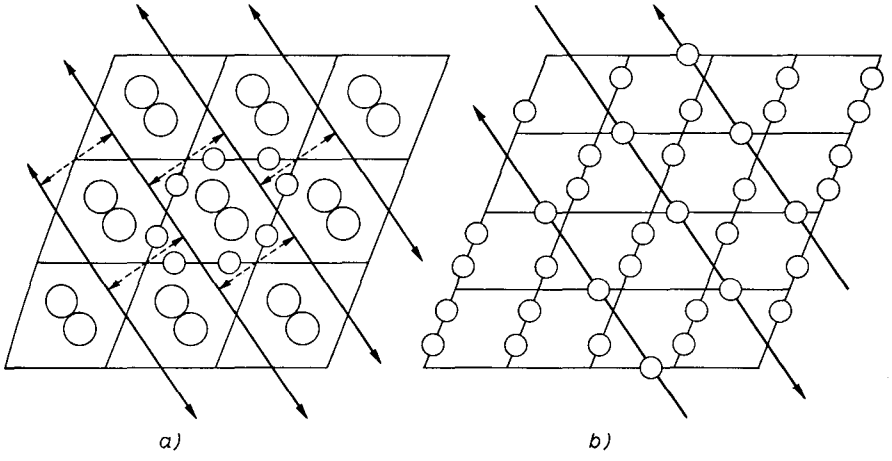

Fig. 7*a*. Map of channels on the plane $y = 0$. Solid arrows mark the centers of continuous eight-membered-ring channels; dashed lines mark ten-membered-ring channels. Solid circles are oxygen atoms

Fig. 7*b*. Map of calcium positions on the plane $y = 0$. Arrows indicate directions of shifts of calcium rows. Not all calcium positions are filled

are linked by sharing oxygen atoms on two sides and by bridging pairs of tetrahedra on the other two sides to form planar sheets normal to the *b* axis. These planar sheets are tied together with four-membered

rings sharing oxygen atoms with the bridging pairs and the structural unit.

Between the planar sheets, continuous channels running parallel to the short cell diagonal in the plane $y = 0$ are formed of eight-membered rings (Fig. 4). Cavities formed of ten-membered rings lie parallel to the long diagonal of the (010) plane (Fig. 5). These cavities are blocked at intervals of 14.8 Å by the four-membered rings which link the structural layers but are intersected by two of the eight-membered-ring channels at right angles. A projection of the structure minus water is shown in Fig. 6*a*. The channels in plan view are shown in Fig. 7*a*. As a result of the two-dimensional channel network, it is possible for cations to move in the plane determined by the structural sheet but ionic migration is precluded in the *b*-axis direction, except perhaps at points of structural defect.

The structure related to morphology

Epistilbite cleaves easily only along the (010) plane, and crystal fragments consist of tightly bonded structural units linked together only by four-membered rings (Fig. 4). The planes parallel to $y = 0$ and $y = 0.50$ pass through the centers of the intersecting systems of channels and cavities and constitute planes of very low bond density. These planes explain the pronounced platy cleavage.

Although the development of well-formed single crystals appears to be extremely rare, natural faces are occasionally developed parallel to (001) and (101). Development of a face parallel to (001) seems to be a result of the high reticular density of atoms of the *C*-centered cell. The angle between the (001) and (101) is 124°20′ which corresponds to the β angle of the unit cell reported by STRUNZ and TENNYSON (1956).

Epistilbite forms roof-shaped twinned crystals such that the (010) normals on each half of the twin subtend an angle of 45°10′. The twin plane corresponds to the $(\bar{1}21)$ and $(\bar{1}\bar{2}1)$ planes of the structure.

The ordering of silicon and aluminum and the cation distribution

The most probable positions of the aluminum atoms became evident during the final stages of refinement. Observed electron densities at the Si sites, including the four-membered ring, were slightly lower than calculated assuming full occupancy by silicon. Electron densitites and curvatures indicated fractional substitution

of .2, .2, .45 for site Si(1), Si(2) and Si(3) respectively. Aluminum-substitution values determined from bond distances differ from the values determined from the electron densities and curvatures. Bond distances related to Si–Al distances given by SMITH and BAILEY (1963) indicate substitution of .3, .0, .35 for Si(1), Si(2) and Si(3) sites respectively. We therefore used adjusted values for .25, .15 and .40.

The distribution of cations Ca and Na follow closely the distribution of aluminum. Calcium positions at .25, .0, .0 and .0, .0, .75, have mean occupancy factors of .16 Ca and .58 Ca respectively. Calculated and observed curvatures of the atomic peaks and electron densities match best when all Na ions are placed in the site .25, .0, .0 but whether all Na occupies the site is speculative. The Ca(1) site which has the highest occupancy lies nearest the Si(3) site with the highest Al substitution. Also the Ca(1) site and its *C*-centered equivalent position result in longer Ca—Ca distances in the *b* direction than the Ca(2) site and its equivalents. The lower Ca—Ca Coulomb repulsion explains greater occupancy in the Ca(1) than in the Ca(2) site. The tilt of the tetrahedra in the four-membered ring is such that Ca—O distances are less at the Ca(1) site than at the Ca(2) site, resulting in larger Coulomb attraction at the Ca(1) site.

That most of the aluminum is not found in the four-membered rings may be accounted for by assuming large Coulomb repulsion introduced by placing aluminum in the four-membered ring even though the four-membered-ring oxygen atoms are closer to the calcium ions.

In studies of silicate layer structures (ROSS and WONES, 1965), streaking of the x-ray film between diffraction spots has been interpreted as indicative of periodic stacking faults in which layers of unit cells are systematically displaced from each other. In layer structures, such as the micas and certain clay minerals, diffuse streaks form continuous or semicontinuous straight lines on precession photographs and connect reciprocal-lattice points along entire festoons in Weissenberg photographs.

Photographs of the epistilbite reciprocal lattice exhibit a diffuse streak connecting the 602, 404 and 206 reciprocal-lattice points as well as other less pronounced bands in the same reciprocal-lattice plane. Although the diffuse line does extend slightly beyond 602 and 206, it does not extend continuously through the reciprocal-lattice row as do streaks from micas or clay minerals.

For epistilbite then, a set of stacks of planes lying parallel to both the short diagonal of the cell in the $y = 0$ plane and the b axis represent the diffuse line found in the reciprocal lattice. The planes are separated by 3.77 Å, and their direction is located by the intersections of the stack of planes 602, 404 and 206 in real space. These planes separate the unit cell into parallel bands containing high concentrations of calcium ion positions. Our interpretation is that the calcium ions are not distributed completely randomly but are partially ordered in a direction normal to the streaked rows in a way which approximates the stacking disorder of micas.

If cell diagonals are drawn passing through the calcium sites on each layer of cations, i.e. $y = 0, 1/2$, then shifts of rows of cations as shown in Fig. 7*b* would account for the major film streaks. Shifted rows should occur more or less randomly on each cation layer and the shifted rows may be of variable length, i.e., from a few unit cells to many cells in length. In addition, four of the water-molecule positions are only partially occupied and will contribute to the streaking effect due to the cation row disorder.

It would be expected that ordering of the calcium and water positions within a given row would cause distortion of the silicate framework near the row and, in particular, would affect the oxygen atoms with the row's coordinates. Since in the structure determination all such distortions are superimposed upon the image of a single unit cell, the positions of the atoms most affected by the distortions or parameter interactions could not refine to single unambiguous positions. The structural oxygen atoms which exhibit abnormal tetrahedral distances are those which lie on planes parallel to the stacking-fault planes, and which include the calcium-ion positions. Since, during the determination of the structure, the same structure was obtained on two sets of independently gathered data, it appears quite likely that the failure of the structure to permit refinement below $R = 0.15$ is partly a function of stacking disorder as well as experimental error in the data.

Coordination of water about calcium ions

Framework oxygen atoms and water molecules form an eight-fold coordination about each Ca ion as illustrated in Fig. 6*b*. Both Ca(1) and Ca(2) sites are coordinated in the same configuration. Four water molecules form a square on one side of each calcium with the plane of the square normal to the *ac* crystallographic plane and parallel to

the long diagonal of the cell. Opposite the square plane of waters, each calcium is bonded to three oxygen atoms and one water molecule. The oxygen atoms and the water molecule form a distorted square plane rotated by 45° to the square plane of water molecules. The sites Ca(1) and Ca(2) differ in coordination only in the bond Ca—O,HOH distances, with the Ca(2) site having longer distances to the framework oxygen atoms in the four-membered ring above and below the $y = 0$ plane. A part of HOH(1), HOH(2), and all of HOH(6) are not associated with Ca ions, but appear to be attached to framework oxygen atoms.

PERROTTA and SMITH (1964) suggest that when cavities in a zeolite are sufficiently large, the exchangeable cations surround themselves by water to form a sphere of hydration, rather than bonding directly to the atoms of the framework. The ten-membered-ring cavities in epistilbite are narrow and long, and the eight-membered-ring channels are distorted and relatively small. It is therefore not possible for spheres of hydration to form around the calcium ions.

Relationship to the Perrotta structure

The structure of our disordered epistilbite differs from the structure of PERROTTA in several respects. The structure of PERROTTA contains only one Ca site, Ca(1), and is thus better ordered than ours. They have found that the entire structure has $C2/m$ symmetry which lessens the tilt of the silica tetrahedra on the $y = 0.2$ and 0.3 levels.

In PERROTTA's structure a water molecule occupies the Ca(2) site giving the Ca(1) site a ninefold coordination of water molecules and framework oxygen atoms. In our structure there seems at most to be but a small amount of water possible on the Ca(2) site—probably not more than about .15 molecules. The disordered structure has a fractional water molecule at 000 whereas the Perrotta structure has none. The Perrotta structure has been tested with our data. The parameters of his framework atoms have been refined to the same values as ours. Electron densities, curvatures, and temperature factors of the Ca and HOH positions are presented in Table 5 for each structure. Although electron densities and curvatures of water positions in both structures may be refined to fit observed values by varying occupancy and temperature factors reasonably, the Ca(1) site cannot contain all the Ca atoms. Their structure causes none of the streaking of the x-ray photographs and therefore does not have

Table 5. *Observed and calculated electron densities and curvatures on cation and water sites in disordered and ordered epistilbite*

	ϱ		$\frac{\partial^2\varrho}{\partial x^2}$		$\frac{\partial^2\varrho}{\partial y^2}$		$\frac{\partial^2\varrho}{\partial z^2}$		B		Occupancy	
	D	O	D	O	D	O	D	O	D	O	D	O
Ca(1)	21.5*	22.2	193.6	204.8	189.1	196.1	155.0	161.0				
	21.6	26.9	189.8	242.1	185.3	234.0	155.6	194.4	2.5	2.5	.58	.74
Ca(2),HOH	7.2	6.9	57.8	53.4	55.3	52.3	41.8	38.4				
	7.2	6.9	54.2	44.5	62.2	53.1	42.5	31.3	2.5,4.4	4.2	.16,.13	0.0,.75
HOH(1)	8.7	7.3	70.9	62.1	74.0	64.9	52.8	44.8				
	8.9	7.5	74.0	62.9	66.4	55.4	54.7	45.1	5.0	5.5	1.0	.92
HOH(2)	8.0	7.1	56.0	51.1	78.4	74.1	52.6	50.7				
	8.0	7.0	54.8	50.0	68.5	60.2	47.7	46.5	4.6	4.8	1.0	.92
HOH(3)	9.2	9.0	41.7	40.1	115.9	110.6	86.7	88.9				
	9.1	9.1	51.5	52.2	98.8	96.7	78.8	85.0	4.4	4.5	1.0	1.0
HOH(5)	6.2	6.7	26.1	27.4	42.7	47.2	48.1	50.1				
	6.2	6.7	34.1	33.0	45.0	47.0	52.0	51.6	4.3	4.4	.70	.75
HOH(4)	5.2		14.1		66.0		33.4					
	5.2		19.2		66.0		36.6		4.5		.50	
HOH(6)	2.4		25.4		18.4		37.3					
	2.4		25.3		14.7		36.1		4.3		.30	
R	.15	.18										
Total HOH	14.9	15.4										

ϱ = electron density at atomic site.
D = disordered structure; O = ordered structure.
* upper value observed, lower value calculated.

the cation-row disorder shown by ours. Disorder increases with increasing crystal intergrowth, as evidenced by more prominent streaking on photographs of single-crystal fragments of intergrown crystals. Probably the amount of disorder varies from the Perrotta structure to equal distribution of Ca,Na on the two cation sites Ca(1), Ca(2). It would appear that the differences between the two epistilbite structures are analogous to differences between a 1M and a 1Md muscovite (SMITH and YODER, 1956, in DEER, HOWIE and ZUSSMAN, 1963).

Acknowledgments

We should like to thank the National Science Foundation for financial support under grant NSF GP 470. We should also like to thank Dr. G. A. JEFFREY and R. SHIONO for the use of the computing facilities at the University of Pittsburgh.

References

W. L. BOND (1942). A mineral survey of piezoelectric materials. Bell System Technical Journal **22**, 145—152 (M.A. 9—115).

W. R. BUSING, K. O. MARTIN and H. A. LEVY (1962), ORFLS, a FORTRAN crystallographic least-squares program. Oak Ridge National Laboratory Report TM-305.

W. A. DEER, R. A. HOWIE and J. ZUSSMAN (1963), *Rock-forming minerals*, vol. 4. John Wiley and Sons, New York.

G. GOTTARDI and W. M. MEIER, The crystal structure of dachiardite. Z. Kristallogr. **119** (1963) 53—64.

E. R. HOWELLS, D. C. PHILLIPS and D. RODGERS (1950), The probability distribution of x-ray intensities. Acta Crystallogr. **3**, 210—214.

IAN S. KERR (1964), Structure of epistilbite. Nature **202**, 589.

W. M. MEIER (1961), The crystal structure of mordenite. Z. Kristallogr. **115**, 439—450.

A. J. PERROTTA (1967), The crystal structure of epistilbite. Min. Mag. **36**, 480—490.

A. J. PERROTTA and J. V. SMITH (1964). The crystal structure of brewsterite. Acta Crystallogr. **17**, 857—862.

M. ROSS and D. R. WONES (1965), Polytypism in biotites. Amer. Mineral. **50**, 291.

M. SLAUGHTER (1964), Structure factor differential Fourier synthesis programs for mineral structures. Technical Report No. 1, Computer Research Center, University of Missouri.

J. V. SMITH and S. W. BAILEY (1963), Second review of Al—O and Si—O tetrahedral distances. Acta Crystallogr. **16**, 801—811.

H. STRUNZ und CH. TENNYSON (1956), „Polymorphie" in der Gruppe der Blätterzeolithe. N. Jahrb. Mineral., Monatshefte, 1—9.